Profiling the Temperature Distribution in AlGaN/GaN HEMTs with Nanocrystalline Diamond Heat Spreading Layers

T.J. Anderson[1], M.J. Tadjer[2], K.D. Hobart[1], T.I. Feygelson[3], J.D. Caldwell[1], M.A. Mastro[1], J.K. Hite[1], C.R. Eddy, Jr[1], F.J. Kub[1], B.B. Pate[1]

1. Naval Research Laboratory, Washington DC 20375, travis.anderson@nrl.navy.mil, 202-404-5854
2. Universidas Politécnica de Madrid, Spain
3. SAIC, Inc, Washington DC 20375

Keywords: wide bandgap, GaN, HEMT, nanocrystalline diamond, raman spectroscopy

Abstract

Reduced performance in Gallium Nitride (GaN)-based high electron mobility transistors (HEMTs) as a result of self-heating has been well-documented. A new approach, termed "diamond-before-gate," is shown to improve the thermal budget of the deposition process and enables large-area diamond without degrading the gate metal. NCD-capped devices had a 20% lower channel temperature at equivalent power dissipation.

INTRODUCTION

As a wide-bandgap semiconductor, gallium nitride (GaN) is attractive for next-generation power converters. The capabilities of GaN-based high electron mobility transistors (HEMTs) to date have been limited by the self-heating effect (reduction of drain current due to lower carrier mobility caused by increased phonon scattering at high drain fields), which has been well-documented in the literature [1-3]. However, attempts to alleviate it have been limited.

Nanocrystalline diamond (NCD) thin-film growth technology has advanced significantly in recent years [4,5]. NCD films possess unique properties, notably high thermal conductivity (up to 1300 W/m-K for t_{NCD} > 3 μm) and very small grain size (~5 nm). Such properties have enabled the growth of smooth (5-25 nm RMS roughness) layers that can act as heat spreading device capping layers. Such schemes in GaN involve growth of AlGaN/GaN on single crystal [6] or CVD [7] diamond, or capping of fully-processed HEMTs using NCD [8], [9]. The bottom-side diamond approaches have faced limitations with substrate size and wafer bow management, while top-side heat extraction using diamond capping of fully-processed AlGaN/GaN HEMTs mandates lower growth diamond temperature, and thus a lower thermal conductivity, due to the presence of a thermally sensitive Schottky gate [8].

EXPERIMENTAL

A new approach has been developed, referred to as "gate after diamond," which enables large-area top-side diamond with high thermal conductivity without risking damage to the Schottky gate [10]. As shown in Figure 1, the diamond is deposited on a thin nucleation dielectric (10 nm PECVD SiN_X) after the mesa and ohmic steps have been completed, but before the gate metal. An O_2-based etch is used to clear the diamond in the gate region before metal deposition. Details of this fabrication sequence can be found elsewhere in the literature [7].

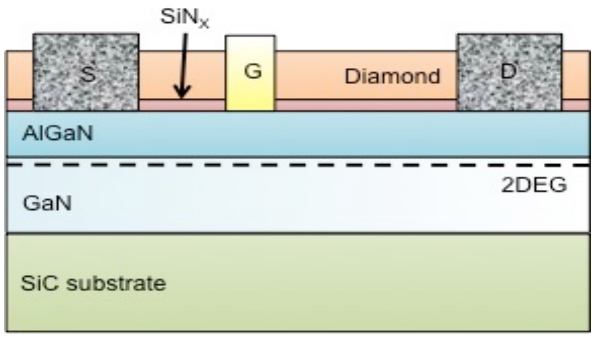

Figure 1. Schematic of AlGaN/GaN HEMT with NCD heat spreading film

Hall measurements on van der Pauw structures were used to characterize the 2DEG at various points in the process to ensure that NCD deposition and processing is not damaging the device. As shown in Table I, it was determined that the diamond deposition alone had minimal impact on the 2DEG. The gate opening process resulted in increased sheet resistance (R_{SH}) and reduced mobility and carrier density. Much of this could be recovered by a short anneal step, implying that this is predominantly plasma damage. To improve the process, a 2-step diamond etch process was developed to enable etching of a relatively thick (0.5 μm) NCD film without plasma damage to the gate region of the device.

TABLE I
HALL MEASUREMENTS ON REFERENCE AND NCD-CAPPED HEMTS

		R_{SH} (Ω/□)	μ (cm^2/V-s)	N_{SH} (cm^{-2})
NCD before gate HEMT	Covered	488	1260	$1.02x10^{13}$
	NCD etch	478	1280	$1.02x10^{13}$
Reference HEMT	Covered	574	1270	$9.22x10^{12}$
	SiN_X etch	533	1270	$8.92x10^{12}$

RESULTS

Electrical characterization of a NCD-capped device has yielded comparable device behavior, as shown in Figure 2. In particular, there was no shift in the threshold voltage, and the sheet resistance, mobility, and 2DEG density was unchanged. It can be inferred qualitatively that the channel temperature is lower in the NCD-capped device based on the lower on-resistance and reduced negative slope in the saturation region.

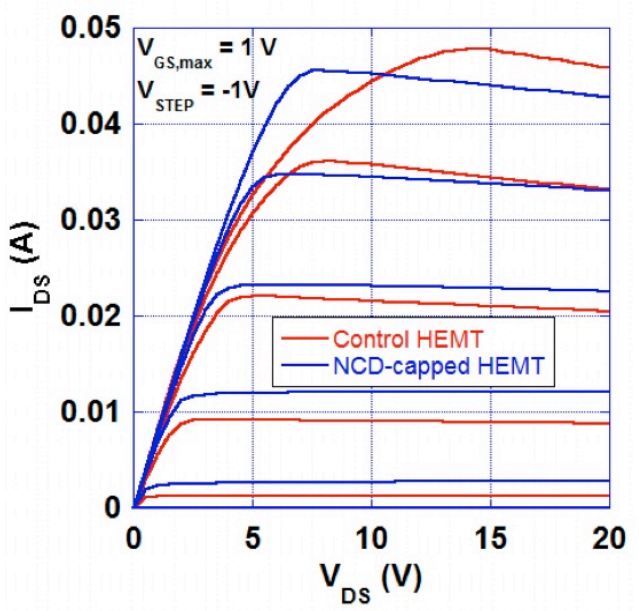

Figure 2. DC I-V curves from a reference and NCD-capped HEMT

To quantify the reduction in channel temperature, the Raman thermography technique was employed [11,12]. A calibration curve fitting the shift in the Raman peak position as a function of temperature was generated by placing the sample on a heated chuck and measuring the Raman spectra over a temperature range of 25-210 °C. After calibration runs on a given device, the laser spot was focused into the region between the gate and drain contacts. During biased testing, the gate voltage was controlled such that $I_{DS} \cong 5$ mA ($V_{GS} \cong$ -1 V), and V_{DS} was increased up to 200 V to yield DC operating power range of 0-10 W/mm.

The shifts in the TO Raman modes were recorded under bias and the Raman shift was used to determine the corresponding rise in device temperature, shown as a function of DC power in Figure 3. The correlation was linear, as expected. At the highest power conditions, the sample with NCD heat-spreading layers exhibited about 20 % lower absolute temperature in comparison to the control HEMT sample. However, the slope of the line for the NCD-capped HEMT is also lower, implying a reduced thermal resistance as well (about 3.75 times lower).

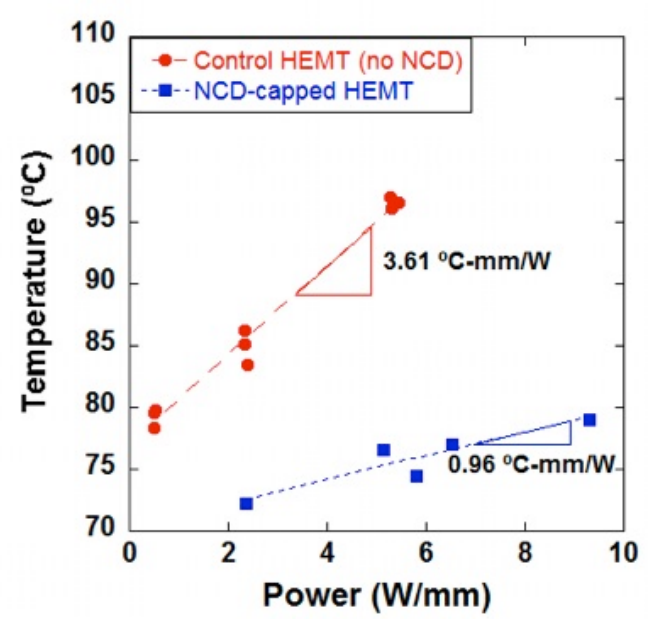

Figure 3. Raman thermography profile of channel temperature with and without NCD heat spreading film.

We have employed a small-diameter collection fiber in an effort to improve the resolution such that the probe area is limited by optical collection volume rather than sample absorption. As a result, we are able to take spectra in ~0.1 μm steps in the vertical direction, enabling us to probe the temperature gradient in much greater detail than has ever been reported. The devices were measured under open gate conditions of V_{DS} = 20V, I_{DS} ~ 90 mA, for a DC power of ~18 W/mm. With the reference and NCD data overlayed, it becomes clear that the temperature gradient is much larger in the active layer of the NCD-capped device, and the substrate temperature is much lower as well. This implies that the NCD layer has effectively changed the heat-sinking of the device to the top surface rather than the bottom surface.

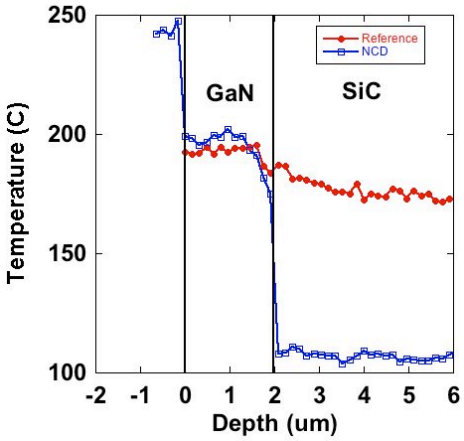

Figure 4. Raman thermography profile of the vertical temperature distribution in the device structure with and without NCD heat spreading film.

CONCLUSIONS

NCD thin film incorporation in AlGaN/GaN HEMTs leads to a reduction of device temperature by 20 % up to 10 W/mm DC power. In addition, NCD-capped devices demonstated improved R_{ON} and N_S. The reduced negative slope of the DC I-V curves provides some limited evidence of reduced self-heating. Raman thermography has further shown a significant reduction in substrate temperature, indicating the device heat sink has become the top surface rather than the substrate. As power and switching frequency increase in next-generation DC/DC converters, more efficient cooling schemes will be necessary. While eventual integration of diamond substrates could revolutionize integrated circuit cooling, we have shown that NCD films can currently cool discrete power transistors.

ACKNOWLEDGEMENTS

The authors are sincerely grateful to Dr. Jeff Calame, Dr. Orest Glembocki, Dr. Steve Binari, Dr. Martin Peckerar, Dr. Martin Kuball, Dr. Michael Mastro, Dr. Jennifer Hite, and the NRL Nanoscience Institute staff..

REFERENCES

[1] J.D. Albrecht, P.P. Ruden, S.C. Binari, and M.G. Ancona, *IEEE Trans. Electr. Dev*., vol. 47, no. 11, pp. 2031, 2000

[2] S. Nuttinck, E. Gebara, J. Laskar, and H.M. Harris, *IEEE Trans. on Microwave Theory and Techniques*, v. 49, no. 12, pp. 2413, 2001.

[3] H.I. Fujishiro, N. Mikami, and M. Hatakenaka, *Phys. Stat. Sol. (c)* 2, no. 7, 2696-2699 (2005).

[4] O. A. Williams, M. Nesladek, M. Daenen, S. Michaelson, A. Hoffman, E. Osawa, K. Haenen, and R.B. Jackman, *Diamond and Relat. Mater*. 17 (2008), 1080-1088 (and references therein).

[5] J.E. Butler and A.V. Sumant, *Chemical Vapor Deposition*, 14, 145 (2008) (and references therein).

[6] M. Alomari, A. Dussaigne, D. Martin, N. Grandjean, C. Gaquiere, and E. Kohn, *Electronics Letters*, vol. 46, 2010, pp. 299-301.

[7] K.D. Chabak, J.K. Gillespie, V. Miller, A. Crespo, J. Roussos, M. Trejo, D.E. Walker, Jr., G.D. Via, G.H. Jessen, J. Wasserbauer, F. Faili, D.I. Babić, D. Francis, and F. Ejeckam, *IEEE Electr. Dev. Lett*., vol. 31, no. 2, pp. 99, 2010.

[8] M. Seelman-Eggebert, P. Meisen, F. Schaudel, P. Koidl, A. Vescan, H. Leier, *Diamond and Relat. Mater*. 10 (2001), 744-749.

[9] M. Alomari, M. Dipalo, S. Rossi, M.-A. Diforte-Poisson, S. Delage, J.-F. Carlin, N. Grandjean, C. Gaquiere, L. Toth, B. Pecz, E. Kohn, *Diamond & Relat. Mater*., vol. 20, pp. 604-608, 2011.

[10] M.J. Tadjer, T.J. Anderson, K.D. Hobart, T.I. Feygelson, J.D. Caldwell, C.R. Eddy, Jr, F.J. Kub, J.E. Butler, B.B. Pate, J. Melngailis. *IEEE Electr. Dev. Lett.* Vol. 33, no. 1 (2012) 23-25

[11] R.J.T. Simms, J.W. Pomeroy, M.J. Uren, T. Martin, M. Kuball, *IEEE Trans. Electr. Dev*., vol. 55, no. 2, pp. 478-482, 2008.

[12] O.J. Glembocki, J.D. Caldwell, J.A. Mittereder, J.P. Calame and S.C. Binari, *Mat. Sci. Forum*, 600-603, 1111 (2009).